

Fenchone, Camphor, 2-Methylenefenchone and 2-Methylenecamphor: A Vibrational Circular Dichroism Study

Giovanna Longhi,[†] Sergio Abbate,^{*,†} Roberto Gangemi,[†] Egidio Giorgio,[‡] and Carlo Rosini[‡]

Dipartimento di Scienze Biomediche e Biotecnologie, Università di Brescia, viale Europa 11, 25123 Brescia, Italy, and Dipartimento di Chimica, Università della Basilicata, via Nazario Sauro 85, 85100 Potenza, Italy

Received: December 9, 2005; In Final Form: February 17, 2006

We report and discuss the infrared (IR) vibrational circular dichroism (VCD) spectra of the enantiomeric pairs of the olefin derivatives of fenchone (1,3,3-trimethyl-2-methylenebicyclo[2.2.1]heptane) and camphor (1,7,7-trimethyl-2-methylenebicyclo[2.2.1]heptane), respectively, together with those of the parent molecules. The VCD spectra were taken in three spectral regions: the mid-IR region, encompassing the fundamental deformation modes, the region of CH-stretching fundamental modes and the NIR-region between 1100 and 1300 nm, which corresponds to the second CH-stretching overtone. The VCD and absorption spectra in the first two regions are analyzed by use of current density functional theory (DFT) calculations. The NIR region is analyzed by a protocol that consists of the use of DFT-based calculations and in assuming local mode behavior: the local mode approach is found appropriate for interpreting the absorption spectra and, for the moment, acceptable for calculating NIR–VCD spectra. The analysis of the first region allows us to track the contribution of the C=O group in the vibrational optical activity of C–C stretching modes; notable differences are indeed found in olefins and ketones. On the contrary, in the other two regions the VCD spectra of olefins and ketones are more similar: in the normal mode region of CH stretching fundamentals the spectra are determined by the mutual orientation of the CH bonds; in the second overtone local mode region olefins and ketones signals show some differences.

I. Introduction

Fenchone (FEN) and camphor (CAM) are two optically active compounds that have been often studied comparatively. They share some properties, but they also show some interesting differences. Both compounds are bicyclic [2.2.1]heptanones of natural origin with the same chemical raw formula $C_{10}H_{16}O$, and both compounds are fairly rigid. Both enantiomers thereof are found as natural compounds and in both cases the most abundant enantiomer is the (1*R*)-one. Yet the optical rotation (OR) at the sodium D-line for the enantiomers with the same Absolute Configuration (AC) in the two molecules is opposite.¹ Other physicochemical properties are different; notably, CAM is a solid up to 175 °C, whereas FEN is a liquid at room temperature.

The investigation of chiroptical properties of these compounds has been conducted for a long time:^{1,2} in particular, the analysis of the circular dichroism (CD) spectrum in the near UV in terms of simple sector rules has necessitated the definition of “octant” and “anti-octant” contributions and the definition of curved nodal planes.^{1,3} A convincing analysis by Pulm et al., based on the comparison of gas-phase CD data and state-of-the-art *ab initio* calculations, allowed to pinpoint contributions from well-defined local moieties to the $n \rightarrow \pi^*$ and $n \rightarrow 3s$ CD bands. In a couple of papers^{4,5} the role of the “helical arrangements of CH_2 groups”⁴ in the cyclopentanonic ring, which is enantiomeric in (1*R*)-fenchone and (1*R*)-camphor, has been shown to be quite special, in addition to the already known role of the substituent

methyl groups encoded in the octant rule. In a study prior to the present one,⁶ the optical rotatory dispersion (ORD) curves in the near UV for CAM and FEN were investigated together with the corresponding curves of the olefin derivatives thereof (1,7,7-trimethyl-2-methylenebicyclo[2.2.1]heptane and 1,3,3-trimethyl-2-methylenebicyclo[2.2.1]heptane, or 2-methylenecamphor and 2-methylenefenchone for short, which we will denote as MECAM and MEFEN, respectively). By comparing data of the olefins and ketones, as well as by critically examining the computational method for calculating ORD, the role and importance of the $n \rightarrow \pi^*$ transitional probabilities, and consequently of the n and π^* orbitals, was evaluated for the ketones. From the same study we learn that the ORD curves at high wavelengths for FEN and MEFEN are the same in sign, whereas they are opposite for CAM and MECAM. We infer that the conclusion in refs 4 and 5 on the perturbing effects of helical structures of rings in the vicinity of chromophores is valid for the electronic states of the C=O group and not for the case of C=C groups.

The present work is concerned with a VCD study of FEN, CAM, MEFEN, and MECAM in three spectral ranges: the mid-IR region (900–1500 cm^{-1}), the CH-stretching region (2800–3000 cm^{-1}), and the second overtone region of the CH-stretching (1300–1100 nm = 7700–9100 cm^{-1}). Related to the above cited papers, we wish to use here VCD with the following two purposes: (i) to find out in which of the three spectroscopic regions of the VCD spectrum just mentioned is there an explicit indication of the special role of the C=O double bond; (ii) to find out in which spectroscopic regions are there some VCD features common to MECAM and CAM or MEFEN and FEN that indicate that vibrational optical activity is originated

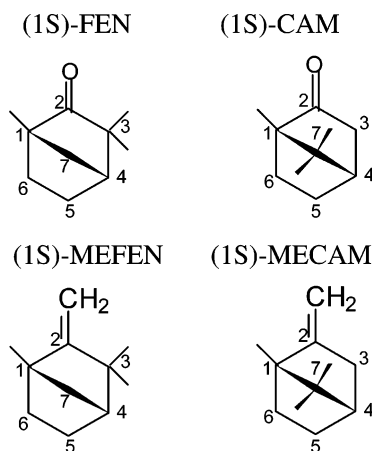
* Corresponding author. E-mail: abbate@med.unibs.it.

[†] Università di Brescia.

[‡] Università della Basilicata.

independently of C=O/C=CH₂ functions. Previous important studies of the VCD spectra of CAM and FEN have been reported:^{7,8} as a matter of fact, ref 7 reports one of the first examples of the application of the protocol devised by Stephens and co-workers,⁹ whereby on rigid molecules the use of VCD experimental data combined with ab initio or DFT calculations allows one to determine for the first time or to confirm the molecular absolute configuration of rigid molecules. Due to the success of the method, VCD has become an increasingly useful tool, after the pioneering work of several groups.^{7–11} As done in ref 7, we have made DFT calculations using the GAUSSIAN-03 package.¹² In Chart 1 below, we report the chemical structures of the (1*S*)-enantiomers of the four molecules under study:

CHART 1



II. Description of Experiments and Calculations

(a) Synthesis of the Olefin Derivatives of Fenchone and Camphor. The enantiomers of FEN and CAM were bought from Sigma-Aldrich and were used without further purification in the spectroscopic experiments described below. The enantiomers of MEFEN and MECAM have been prepared as previously reported.^{6,13} We wish to report here the values of optical rotation (OR) at the sodium D-line measured at RT: for (1*S*)-MEFEN, $[\alpha]_D = +71$ (*c* 1.05, hexane); for (1*R*)-MEFEN, $[\alpha]_D = -68$ (*c* 1.08, hexane); for (1*S*)-MECAM, $[\alpha]_D = +37$ (*c* 0.96, hexane); for (1*R*)-MECAM, $[\alpha]_D = -34$ (*c* 1.03, hexane). We recall from the Aldrich catalog that neat (1*R*)-FEN has $[\alpha]_D = -50.5$, neat; (1*S*)-FEN has $[\alpha]_D = +60$, neat; (1*R*)-CAM has $[\alpha]_D = +44$ (*c* 10, ethanol); and (1*S*)-CAM has $[\alpha]_D = -43$ (*c* 10, ethanol).

(b) VCD and Absorption Spectra: Mid-IR Region. The spectra were taken on the following solutions: for both enantiomers of FEN, 1.2 M/CCl₄; for both enantiomers of CAM, 1.2 M/CCl₄; for both enantiomers of MEFEN, 3 M/CCl₄; for both enantiomers of MECAM, 3 M/CDCl₃. The solutions were placed in 0.05 mm path length BaF₂ cells and the VCD spectra were taken on a JASCO FVS4000 FTIR instrument equipped with an MCT detector; 2000 scans were taken for both enantiomers, and mirror image appearance was obtained for them. In Figure 1 we report the absorption and VCD spectra of FEN and MEFEN, together with the results of the calculations discussed below. In Figure 2 we report the absorption and VCD spectra of CAM and MECAM, together with the results of the calculations discussed below. In all cases the reported VCD data are one-half the difference of the two VCD spectra of enantiomer (*S*) and (*R*) and are thus to be associated with the (1*S*)-

enantiomers.¹⁴ The frequency range is between 900 and 1500 cm⁻¹, for all molecules except for MECAM (1500–920 cm⁻¹), because the spectra for the latter compound were taken in CDCl₃, which has an absorption band at ca. 900 cm⁻¹. The ordinate axes are in ϵ and $\Delta\epsilon$ for absorption and VCD, respectively.

(c) VCD and Absorption Spectra: CH-Stretching Region. The spectra were taken on the following solutions: for both enantiomers of FEN, 0.3 M/CCl₄; for both enantiomers of CAM, 0.4 M/CCl₄; for both enantiomers of MEFEN, 0.3 M/CCl₄; for both enantiomers of MECAM, 0.33 M/CDCl₃. The solutions were placed in 0.05 mm path length BaF₂ cells and the VCD spectra were taken on a JASCO FVS4000 FTIR instrument equipped with an InSb detector; 10 000 scans were taken for both enantiomers, with 8 cm⁻¹ resolution. In Figure 3 we report the absorption and VCD spectra of FEN and MEFEN, together with the results of the calculations discussed below. In Figure 4 we report the absorption and VCD spectra of CAM and MECAM, together with the results of the calculations discussed below. As for the mid-IR region, the reported VCD spectra are obtained from the averages of the VCD spectra of (*R*)- and (*S*)-enantiomers; i.e., they are obtained from $((S) - (R))/2$.¹⁴ In all cases the frequency range is between 2800 and 3050 cm⁻¹. The ordinate axes are in ϵ and $\Delta\epsilon$ for absorption and VCD, respectively.

(d) VCD and Absorption Spectra: NIR Region. In Figure 5 we give the NIR absorption and NIR-VCD spectra in the region 1100–1300 nm of both enantiomers of FEN, CAM, MEFEN, and MECAM; the reported VCD spectra are presented as superimposed, but we give the absorption spectrum of just one enantiomer. The NIR-VCD spectra in the second overtone region (1300–1100 nm) of both enantiomers of FEN, and of both enantiomers of CAM were first reported in refs 15 and 16, where our homemade experimental dispersive apparatus and the procedure to obtain NIR-VCD spectra are described; we show them here for completeness. Both enantiomers of FEN were used as neat liquids (ca. 6.23 M) in 5 mm path length quartz cells; both enantiomers of CAM were measured on a 2.6 M solution of CCl₄ in 5 mm quartz cells. The enantiomers of MEFEN were treated similarly to those of FEN; namely, they were used neat in 5 mm quartz cells (to evaluate ϵ and $\Delta\epsilon$ the density of fenchone has been assumed); the enantiomers of MECAM were dissolved in CCl₄ with 2.8 and 3 M concentration for the two enantiomers (1*S*) and (1*R*), respectively, and NIR-VCD spectra were taken in 5 mm quartz cells.

The procedure followed to take NIR-VCD spectra is described in ref 16, and succinctly, we may say that it consists of taking a number of CD spectra from 2 to 4, subtracting out polarization artifacts that vary with varying absorbance, as obtained by measuring spectra with the sample cell placed between the linear polarizer and the photoelastic modulator, and by finally dividing by the dc signal, which is provided by our apparatus. Notice that CAM NIR-VCD spectrum compares well with the FTNIR-VCD result obtained by Cao et al.¹⁷

(e) Calculations. As mentioned above, ab initio/DFT calculations have been used to get an interpretation of the experimental results presented in Figures 1–5. We have employed the GAUSSIAN03 platform,¹² and a JASCO FVS4000 software that allows easy comparison of experiment and calculations. For the *mid-IR* and *CH-stretching* regions we worked as suggested in the literature and in particular as already done for FEN and CAM.⁷ We tried the functionals/basis sets B3LYP/6-31G** and B3PW91/TZVP. Comparable results were obtained for the two cases except for a quite characteristic negative VCD doublet

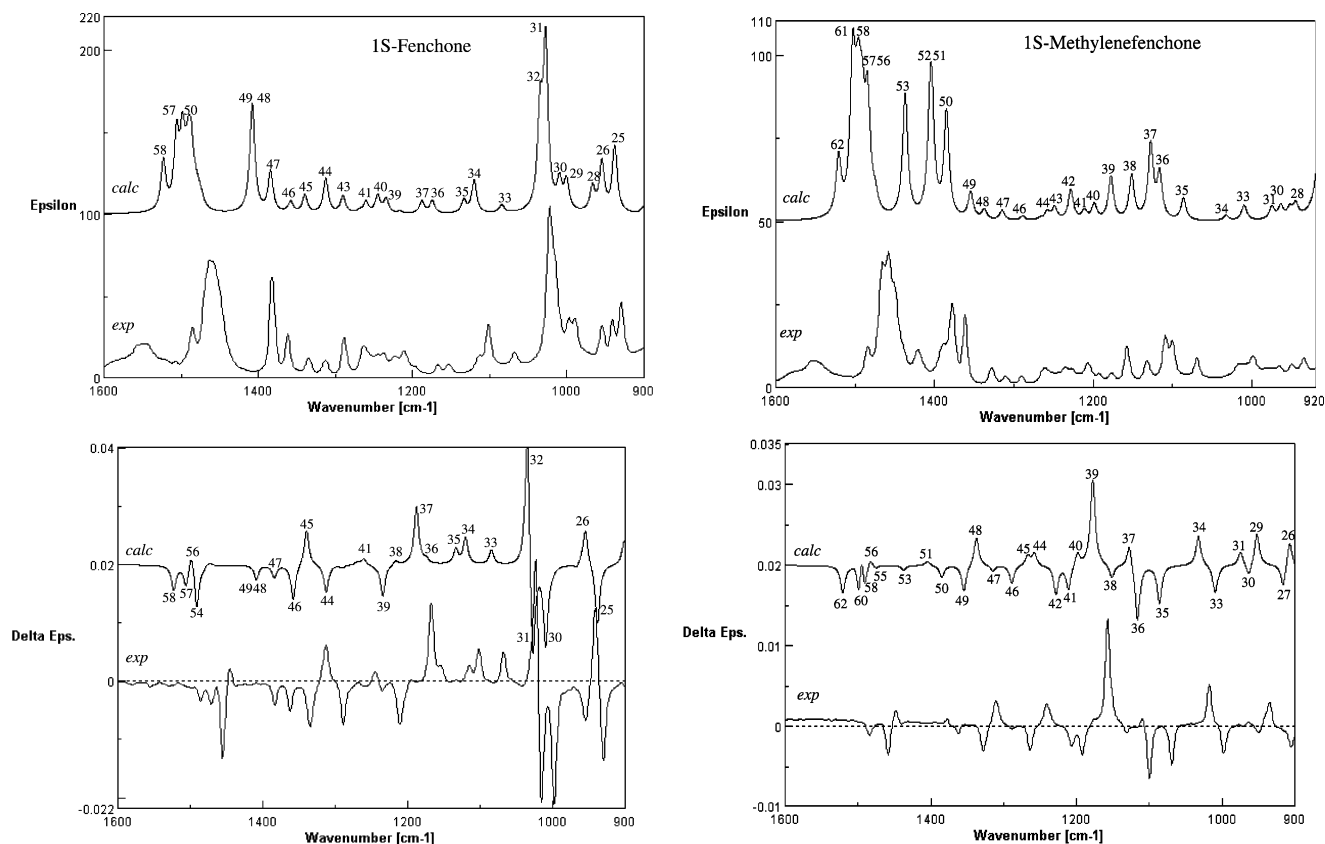


Figure 1. Experimental and calculated absorption and VCD spectra in the mid-IR (900–1500 cm^{-1}) of (1*S*)-fenchone (FEN) (left) and of (1*S*)-2-methylenefenchone (MEFEN) (right). The experimental VCD spectra are obtained from the VCD spectra of (1*R*)-enantiomer and (1*S*)-enantiomer, as explained in the text. The calculated absorption and VCD spectra are obtained from calculated frequencies, dipole strengths, and rotational strengths (B3PW91/TZVP), by assigning a Lorentzian shape to bands of 4 cm^{-1} HWHH. The numbering on the calculated spectra indicates normal modes illustrated in Table 1.

observed in FEN at ca. 1000 cm^{-1} . For this reason we report just the results for B3PW91/TZVP: in Table 1 we give the calculated frequencies, dipole strengths, rotational strengths, and a rough mode description for the vibrational normal modes in the mid-IR of the four molecules as deduced from GAUSSVIEW.¹² The numbering of Table 1 is then used to label the calculated features of Figures 1 and 2, where we give the calculated results in graphical terms, by assigning a Lorentzian shape to the calculated bands of given center-frequency and dipole (rotational) strengths with $\gamma = 4 \text{ cm}^{-1}$, without any scaling factor, and we superimpose the calculated spectra to experimental ones, to facilitate comparison. In Table 2 we give the corresponding results of the calculations in the CH-stretching region; analogously to what was done in the mid-IR region; we also produce the graphical representation of the calculations, by assigning Lorentzian band shapes with $\gamma = 8 \text{ cm}^{-1}$ to each calculated feature and superimpose the calculated absorption and VCD spectra to experimental ones in Figures 3 and 4, shifting the frequencies by 134 cm^{-1} : this is provided by the software of JASCO FVS 4000 and has the same effect as an ad hoc multiplicative factor that is currently used.^{8,14} For the NIR region, B3LYP/6-31G** calculations have been done, following a procedure already used in ref 16. The basic assumption is that in the considered spectral region, corresponding to the $\Delta\nu = 3$ overtones of CH-stretchings, only local modes are present.^{16,18} For this reason we have performed $n = 16$ calculations for FEN and CAM, and $n = 18$ calculations for MEFEN and MECAM, whereby $(n - 1)$ hydrogen atoms are ^2H isotopes and one is a ^1H isotope. Out of these calculations we take n values for the calculated harmonic frequencies ω_0 , for the dipole strengths D , and for the rotational strengths R of

isolated CH-stretchings: these values represent the local modes at $\Delta\nu = 1$. We transfer them to $\Delta\nu = 3$ as follows. The values of D and R are used as they are: this means that the relative values of D and R for the n local mode transitions are assumed to be the same in the $\Delta\nu = 1$ as in the $\Delta\nu = 3$ (and further) region. For D this is seen approximately to be the case, as of local mode intensity studies;^{19–22} for R this is a mere assumption. Finally, we evaluate the ω_{0-3} values in the $\Delta\nu = 3$ region from the Birge–Sponer relation:^{19,20}

$$\omega_{0-3} = 3(\omega^{\text{h}} - \chi) - 9\chi$$

where ω^{h} is the harmonic frequency and χ is the anharmonicity constant. In ref 16 ω^{h} were assumed to coincide with the ab initio calculated values for ω_0 , and a value for $\chi = 70 \text{ cm}^{-1}$ for all CH bonds was taken; an excellent almost quantitative prediction of the experimental absorption spectrum was obtained and an almost acceptable qualitative interpretation of the VCD spectrum was achieved. The same procedure was followed, with similar success for α - and β -pinenes.²³ In the present case though, we recognize that the chosen absolute value for χ is somewhat high as compared to the experimental values of the literature for cyclic²⁴ and noncyclic ketones,²⁵ as well as for cyclic hydrocarbons such as cyclohexane:²⁴ indeed a value $\chi = 65 \text{ cm}^{-1}$ seems more adequate for these compounds and we have taken here this value for the present work. For the same reason we took $\chi = 55 \text{ cm}^{-1}$ for the olefin CHs, as of the studies of propylene,²⁵ butenes²⁶ and cycloalkynes.²⁷ In the latter triad of papers,^{25–27} the values $\chi = 60 \text{ cm}^{-1}$ are deduced for methyl CHs or non olefin CHs close to the C=C double bond: such a value was used for the two CH bonds in position 3 in MECAM.

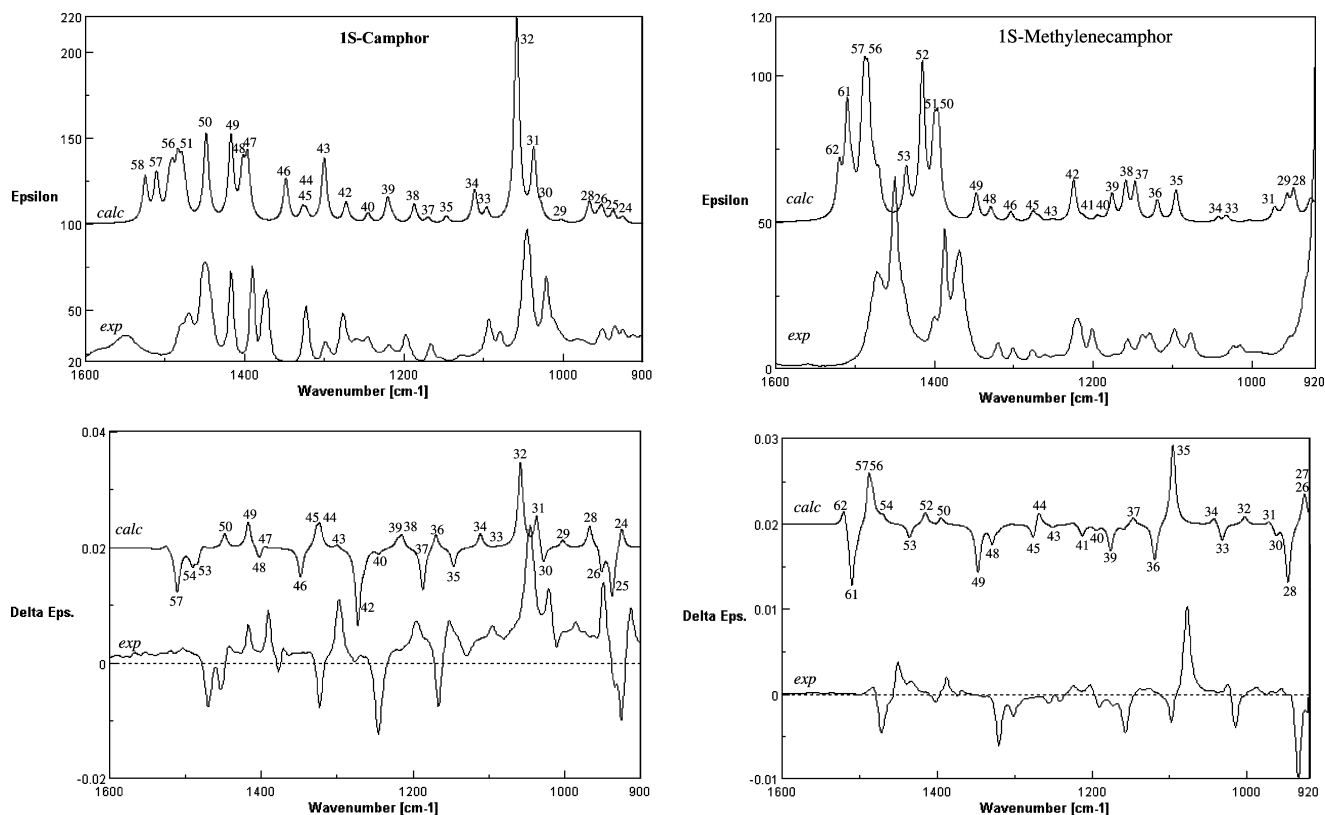


Figure 2. Experimental and calculated absorption and VCD spectra in the mid-IR (900–1500 cm^{-1}) of (1*S*)-camphor (CAM) (left) and of (1*S*)-2-methylenecamphor (MECAM) (right). The experimental VCD spectra are obtained from the VCD spectra of (1*R*)-enantiomer and (1*S*)-enantiomer, as explained in the text. The calculated absorption and VCD spectra are obtained from calculated frequencies, dipole strengths, and rotational strengths (B3PW91/TZVP), by assigning a Lorentzian shape to bands of 4 cm^{-1} HWHH.

The results are summarized in Table 3 (λ values are obtained from $\omega_{0 \rightarrow 3}$ in the above Birge–Sponer equation). In Figure 6 we report the graphical representation of the results for the (1*S*)-enantiomers, where each one of the n transitions is represented by a Lorentzian band centered at the calculated λ -value, with integrated area equal to either D or $|R|$, and with $\gamma = 10$ nm for all transitions. The calculated spectra are the superpositions of these Lorentzian traces. The results are presented in the same order as done in Figure 5 for the experimental results, namely, in the top left square we have the result for (1*S*)-FEN, in the top right one those for (1*S*)-CAM, in the bottom left one those for (1*S*)-MEFEN, in the bottom right one those for (1*S*)-MECAM.

III. Discussion of the Results

The study of all three investigated regions allows one to get useful information about the absolute configuration of the molecules and/or the role played by chemical groups within the molecules. Below we discuss the three regions in order of increasing frequency.

(a) Mid-IR Region. In this region and for this type of rigid molecules the comparison of DFT and experimental data is expected to be quite satisfactory for both absorption and VCD spectra.^{7,9} This is indeed the case even for MEFEN and MECAM that, to our knowledge, had not been investigated previously. From the comparison of the results of FEN and MEFEN and CAM and MECAM, we may notice a few interesting facts, which are explained on the basis of the calculations.

(i) The intensities, both in absorption and in VCD, are generally larger for FEN than for MEFEN and for CAM than for MECAM;

(ii) The largest differences in this respect are noticed in the group of two bands observed in absorption spectra of FEN and CAM just above 1000 cm^{-1} , which are not observed in MEFEN and MECAM. To those intense absorption bands there correspond large experimental intense VCD features in FEN and CAM, whereas correspondingly VCD features in MEFEN and MECAM are quite weak. On the other extreme frequency side of absorption and VCD spectra, at ca. 1450 cm^{-1} , the behavior of MEFEN and FEN and of MECAM and CAM is more similar. The analysis of normal modes in Table 1 and Figures 1 and 2 allows one to get some clue onto understanding the reason for these intensity differences. It is indeed observed that features 31 and 32, which are the particularly intense lines just mentioned for FEN and CAM, are due to CC-stretchings close to the C=O bond; the corresponding modes in MEFEN and MECAM are for CC-stretchings close to the C=CH₂ group: they have similar frequencies and they are rather weak. On the contrary, the features at ca. 1450 cm^{-1} are due to HCH bendings and are less influenced by the nearby C=O or C=CH₂ group, resulting in more similar spectra in the olefins and ketones. The strong influence of the oxygen atom on the absorption and VCD spectra is not just typical of the C=O group but is also observed for the *endo*-COH group in borneol²⁸ and fenchyl alcohol;²⁹ the same phenomenon is also observed in sugar molecules, especially in α -anomers of aldohexoses, where a group of VCD features between 1000 and 1100 cm^{-1} has been suggested to monitor the anomeric status.^{30,31}

(b) CH-Stretching Region. The most interesting feature of this region is that, overall, the VCD spectrum of FEN is opposite to that of CAM for the same absolute configuration of the stereogenic carbon atom 1. Here we can add further facts that may allow some general use of the VCD data in the CH-

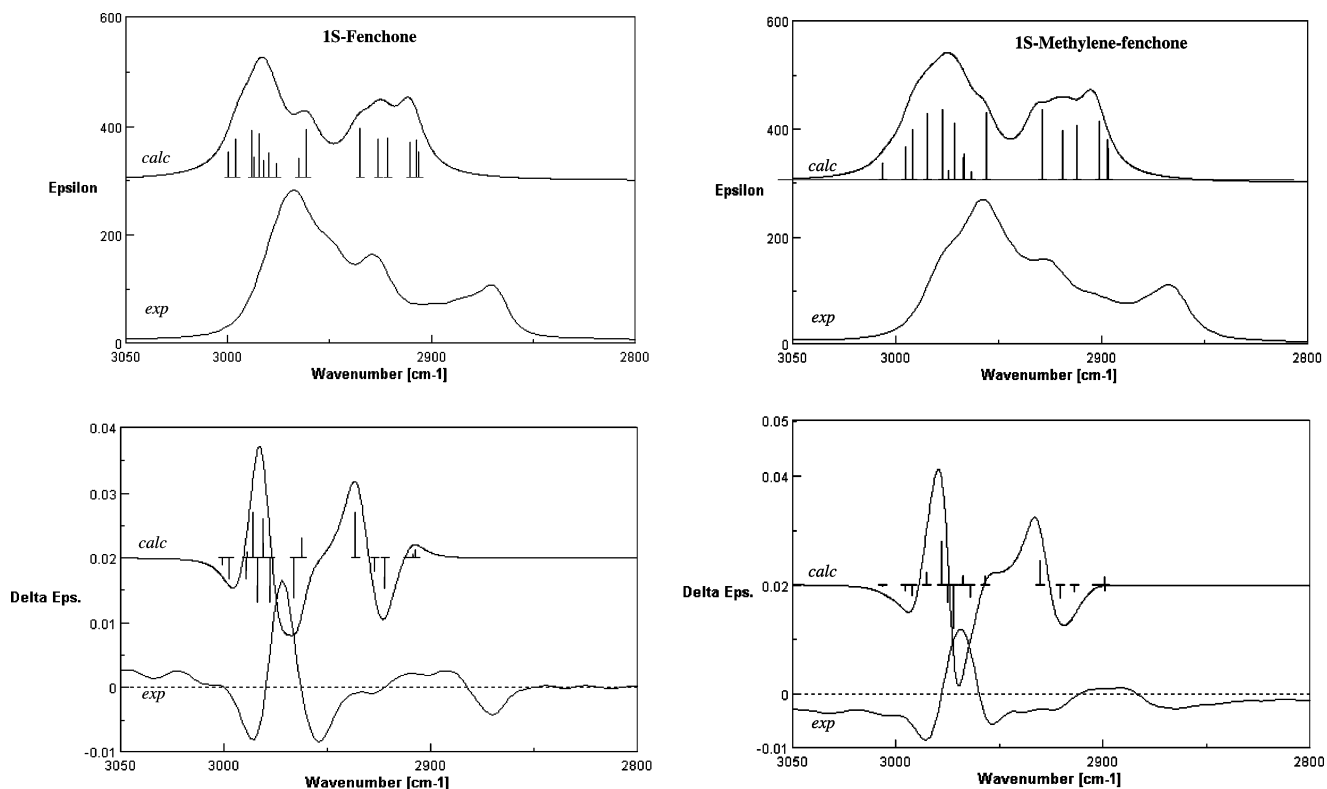


Figure 3. Experimental and calculated absorption and VCD spectra in the IR range of CH-stretching fundamentals (2700–3050 cm^{-1}) of (1S)-fenchone (FEN) (left) and of (1S)-2-methylfenchone (MEFEN) (right). The experimental VCD spectra are obtained from the VCD spectra of (1R)-enantiomer and (1S)-enantiomer, as explained in the text. The calculated absorption and VCD spectra are obtained from calculated frequencies, dipole strengths, and rotational strengths (B3PW91/TZVP), by assigning a Lorentzian shape to bands of 8 cm^{-1} HWHH; spectra have been shifted by 134 cm^{-1} (see text). Bars superimposed to the calculated spectra are located at calculated frequencies and are proportional to calculated dipole and rotational strengths.

stretching region for [2.2.1] bicyclic molecules. First, from Figures 3 and 4 one may also see that, to a first approximation, the same is true for MEFEN and MECAM. Indeed, although in (1S)-FEN one has a clear triplet of VCD bands with alternating signs ($-$, $+$, $-$) at ca. 2980, 2965, and 2955 cm^{-1} , respectively, followed by a broad ($+$)-VCD feature at ca. 2900 cm^{-1} , in (1S)-CAM one has a VCD-triplet ($+$, $-$, $+$) at ca. 2980, 2960, and 2945 cm^{-1} , followed by a broad ($-$)-VCD feature at ca. 2900 cm^{-1} (see Figures 3 and 4). At the same time for (1S)-MEFEN one has a ($-$, $+$, $-$)-VCD triplet at ca. 2975, 2965, and 2950 cm^{-1} (the last negative feature is rather weak) followed by a ($+$) broad VCD band at 2900 cm^{-1} . In (1S)-MECAM one has a ($+$, $-$, $+$) VCD triplet at 2980, 2960, and 2940 cm^{-1} followed by a broad ($-$)-VCD feature at ca. 2900 cm^{-1} (the highest frequency feature is here the less intense one). Second, the calculated spectra, even though not perfect, are in fair agreement with the experimental data and are, to a certain extent, useful to draw some conclusions. The calculated VCD bands are consistent with the observed features at high frequencies, whereas below 2900 cm^{-1} the matching of experiment and theory is less convincing, even for absorption data; indeed, there is more than a suspect here that the anharmonic phenomenon of Fermi resonance (FR) is perturbing the CH_2 -stretching symmetric normal modes³² that are calculated in the lowest part of the CH-stretching region (see Table 2). Accounting for FR is beyond the level of calculations of current computational facilities for VCD.^{9,12} The CH_2 -antisymmetric stretching normal modes, whose frequencies have higher values than those of the CH_2 -stretching symmetric normal modes, are unaffected by FR for local symmetry reasons and the matching of theory and experiment is consequently much better. Triplets of calculated VCD bands of alternating signs are indeed found

in the region of CH_2 -antisymmetric stretching normal modes (see Figures 3 and 4). However, it is not possible to assign the individual bands in the calculated triplets to well-defined delocalized CH_2 or CH_3 antisymmetric normal modes. Indeed, we observe that the VCD and absorption bands are superpositions of several features (sometimes of different signs); in trying to sort out the major contributions to the VCD bands from Table 2, we may say that, starting from the high-frequency side, we have the following group contributions (the numbering refers to the current IUPAC numbering of molecules, presented in Chart 1):

	FEN and MEFEN		CAM and MECAM
VCD band	of $-$ sign	ca. 2980 cm^{-1}	of $+$ sign
groups involved	3		7
VCD band	of $+$ sign	ca. 2960 cm^{-1}	of $-$ sign
groups involved	1, 3, 7		1, 5, 6
VCD band	of $-$ sign		of $+$ sign
groups involved	4, 5, 6	ca. 2950 cm^{-1}	4, 5, 6

According to these attributions, we conclude and propose that the VCD in FEN/MEFEN being opposite to that in CAM/MECAM is not by chance and is due to the fact that the moiety $\text{CH}_2(6)\text{CH}_2(5)[\text{C}^*\text{H}(4)]\text{CH}_2(7)(\text{CH}_3)_2(3)$ generating the largest part of the ($-$, $+$, $-$) triplet in FEN/MEFEN is approximately enantiomeric to the moiety $\text{CH}_2(6)\text{CH}_2(5)[\text{C}^*\text{H}(4)]\text{CH}_2(3)-(\text{CH}_3)_2(7)$ that generates the ($+$, $-$, $+$) VCD triplet in CAM/MECAM. $\text{C}^*\text{H}(4)$ contributes significantly just to the pair CAM and MECAM and for that reason we have reported it in brackets (see Chart 2). (Also $\text{CH}_3(1)$ seems to contribute a little, but we exclude it for the time being.)

The mirror-image appearance of VCD spectra of FEN/MEFEN and CAM/MECAM, being related to the spatial

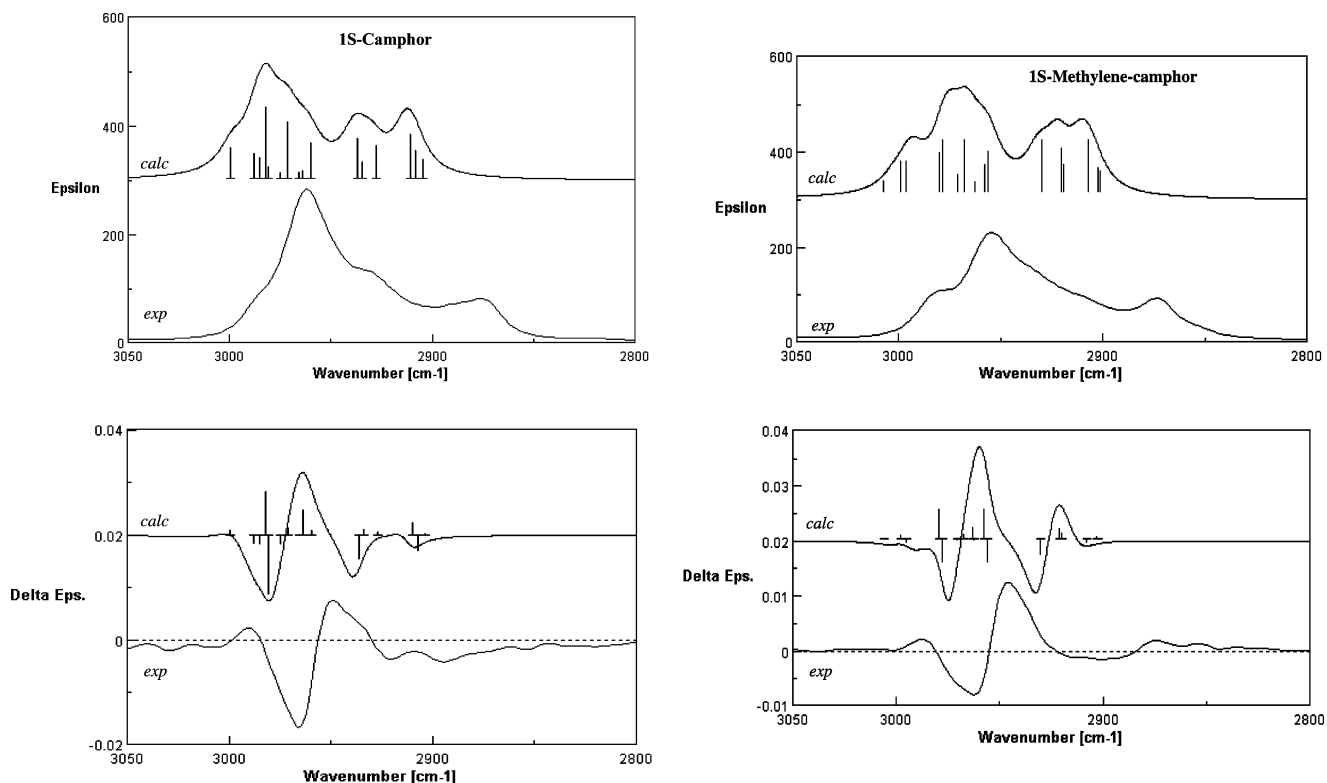
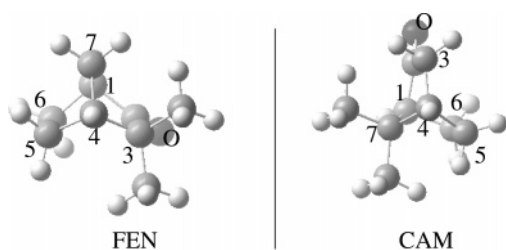


Figure 4. Experimental and calculated absorption and VCD spectra in the IR range of CH-stretching fundamentals (2700–3050 cm^{-1}) of (1*S*)-camphor (CAM) (left) and of (1*S*)-2-methylenecamphor (MECAM) (right). The experimental VCD spectra are obtained from the VCD spectra of (1*R*)-enantiomer and (1*S*)-enantiomer, as explained in the text. The calculated absorption and VCD spectra are obtained from calculated frequencies, dipole strengths, and rotational strengths (B3PW91/TZVP), by assigning a Lorentzian shape to bands of 8 cm^{-1} HWHH; spectra have been shifted by 134 cm^{-1} (see text). Bars superimposed to the calculated spectra are located at calculated frequencies and are proportional to calculated dipole and rotational strengths.

CHART 2



arrangement of local moieties in the molecules, is reminiscent of the explanation of electronic CD data recalled in the introduction of this paper but does not have to do with the C=O group, which in refs 4 and 5 was important. The generation of VCD is here due to a moiety formed by $\text{CH}_2\text{-C}^*\text{H-(CH}_3)_2$ groups arranged in a chiral manner, most probably interacting like vibrational excitons, as was proposed a long time ago for the chiral $\text{CH}_2\text{CH}_2\text{C}^*\text{H}$ fragment found in some twenty monoring molecules.^{23,33} For this reason we feel confident to find similar behavior in similar molecules: indeed, in (1*S*)-borneol we find the same behavior as in (1*S*)-CAM and in (1*R*)-fenchyl alcohol as in (1*R*)-FEN.²⁹ Other examples of well defined [2.2.1] bicyclic molecules had been studied jointly by Moscovitz, Lightner and Pultz in 1982.³⁴

(c) NIR Region. If one compares the results of Figure 6 with those of Figure 5, one can still maintain the general judgment drawn in the conclusions of ref 16, namely the prediction of the absorption spectra by the proposed method is quite good, as far as the general shape is concerned, and the calculation of the VCD overtone spectrum is acceptable for the time being. Let us now first get to a more detailed examination of the *NIR-absorption spectra*: the main feature for CAM and MECAM

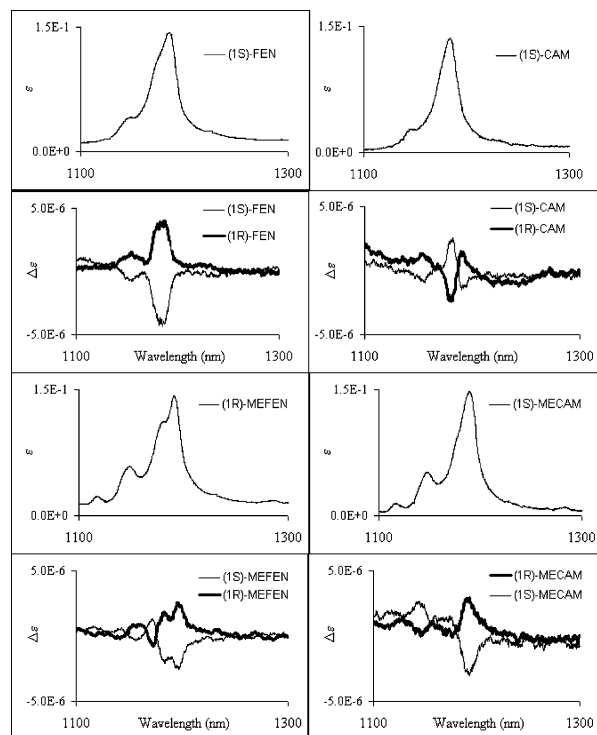


Figure 5. Experimental absorption and VCD spectra in the NIR (1300–1100 nm) of (1*S*)-fenchone (FEN) and (1*R*)-fenchone (top left), of (1*S*)-camphor (CAM) and (1*R*)-camphor (top right), of (1*S*)-2-methylenefenchone (MEFEN) and (1*R*)-2-methylenefenchone (bottom left), and of (1*S*)-2-methylenecamphor (MECAM) and (1*R*)-2-methylenecamphor (bottom right). For experimental details, see text.

TABLE 1: Calculated Frequencies ω (cm^{-1}), Dipole Strengths D (10^{-40} $\text{esu}^2 \text{cm}^2$), Rotational Strengths R (10^{-44} $\text{esu}^2 \text{cm}^2$) and Mode Assignments for Fenchone, Methylene-fenchone, Camphor, and Methylene-camphor in the Region 1600–900 cm^{-1} ^a

no.	ω	D	R	assignment	no.	ω	D	R	assignment
Fenchone									
58	1522.96	22.00	-7.53	3, 5b, 6b	40	1245.23	9.49	-0.51	C2–C3
57	1505.97	32.22	-6.55	3, 6b, 7b	39	1234.37	7.89	-12.24	C3–C4
56	1498.46	29.40	5.77	3, 5b, 6b, 7b	38	1216.38	1.19	1.56	?
55	1494.81	5.01	0.58	1, 3, 5b, 6b, 7b	37	1187.92	6.93	23.17	?
54	1491.04	19.32	-14.55	1, 3, 7b	36	1174.56	7.25	1.86	?
53	1487.23	24.34	0.47	1, 3, 5b, 6b, 7b	35	1133.56	7.50	6.19	?
52	1481.97	6.54	-0.78	1	34	1120.26	19.68	11.18	4, 5t, 6t, 7t
51	1477.42	5.92	0.69	3, 5b, 6b	33	1084.53	5.07	6.19	1, 4, 5t, 6t, 7t
50	1473.05	3.13	0.88	3	32	1034.8	60.25	69.08	?
49	1408.43	21.52	-7.31	1, 3	31	1027.59	108.57	-54.32	C2–C1
48	1407.38	31.85	2.61	1, 3	30	1009.55	18.53	-37.84	?
47	1384.13	19.96	-4.25	3	29	1000.49	20.00	-1.76	?
46	1358.03	5.48	-12.36	C1–CH3	28	966.958	16.76	-1.99	C5–C6
45	1339.67	9.06	12.85	4	27	958.331	0.92	2.35	3
44	1312.5	17.91	-10.03	5r	26	954.577	34.36	17.34	C7–C4
43	1290.34	8.93	-1.00	4, 6t, 7t	25	937.937	47.83	-30.34	?
42	1269.08	1.32	1.15	4, 5t, 6t, 7r	24	901.121	2.98	14.05	?
41	1260.47	6.03	2.35	7r					
Camphor									
58	1525.09	18.29	1.56	5b, 7	40	1245.09	5.13	-1.71	5t, 6r
57	1510.96	18.80	-13.51	6b, 7	39	1220.29	13.09	2.91	3t, 4, 5w, 6t
56	1507.20	1.00	-0.95	5b, 7, 1	38	1214.54	2.44	4.66	3r, 4, 5t
55	1494.90	12.63	-0.75	5b, 6b, 7, 1	37	1186.97	10.33	-17.41	C–C (?) stretch 3t, 4, 5t, 6t
54	1490.70	14.60	-4.54	5b, 6b, 7, 1	36	1169.91	2.91	6.33	5t, 6w
53	1484.18	19.19	-4.20	5b, 6b, 7, 1	35	1146.54	3.88	-7.87	3t
52	1478.86	17.51	1.23	3b, 5b, 7, 1	34	1111.08	18.78	5.91	3t, 5t, 6t
51	1475.08	7.74	0.66	5b, 6b, 7, 1	33	1096.02	7.40	-0.26	3t, 5t, 6t
50	1448.38	38.59	4.71	3b	32	1058.18	124.29	38.44	C2–C3 stretch, 5t, 6t
49	1417.24	37.94	8.97	7, 1	31	1036.85	43.20	14.77	?
48	1402.65	20.86	-4.15	1	30	1028.04	5.48	-9.33	4, 7
47	1396.48	26.60	1.26	7	29	1002.34	1.76	3.54	7
46	1348.27	21.23	-10.58	C1–CH3 stretch, 6r	28	967.02	14.10	11.44	4, C5–C6
45	1327.28	5.81	5.33	5r, 4	27	955.90	3.60	4.00	7
44	1322.73	4.09	7.08	5t, 4, 3r	26	951.44	10.39	-13.03	4, C5–C6
43	1300.04	32.10	1.37	?	25	937.13	8.06	-25.55	3w
42	1272.55	10.30	-28.78	3t, 5t, 6t, 4	24	924.82	4.51	12.02	C4–C7
41	1264.49	0.68	-4.25	3r, 4, 5					
Methylene-fenchone									
62	1520.89	12.47	-6.11	3, 5b, 6b, 7b	43	1248.6	3.37	-0.25	4, 5t, 6r, 7t
61	1503.17	31.78	1.22	3, 6b, 1	42	1228.17	8.27	-7.98	4, 5t, 6t, 7t
60	1498.24	9.90	-9.95	1, 3	41	1211.06	2.49	-7.19	?
59	1495.45	17.14	8.55	1, 3, 5b	40	1198.6	4.28	3.51	?
58	1491.07	17.72	-5.88	1, 3, 7b	39	1177.64	12.29	25.10	?
57	1484.61	19.69	0.19	1	38	1151.44	12.69	-4.15	?
56	1483.17	5.22	1.75	6b	37	1127.39	22.17	7.25	=CH2 w
55	1475.25	2.61	-0.74	3, 5b	36	1116.2	13.39	-17.44	?
54	1473.85	0.80	0.18	1, 7b	35	1086.12	6.75	-11.96	7t
53	1437.01	28.57	-1.17	=CH2 b	34	1032.66	1.71	10.02	C5–C6
52	1405.52	19.53	0.73	3	33	1009.78	4.95	-9.17	?
51	1403.34	19.91	0.41	1	32	1005.27	0.25	-0.83	3
50	1384.83	25.44	-2.93	3	31	974.71	4.32	4.86	C5–C6, 7w, 1
49	1354.46	6.57	-6.59	C1–CH3, 6r, 7r	30	963.44	4.42	-4.62	C7–C4
48	1337.35	2.50	7.34	4	29	952.27	3.40	11.70	?
47	1314.7	2.45	-1.57	5r	28	944.74	4.78	0.09	?
46	1288.85	1.09	-4.80	4	27	916.13	7.93	-8.90	C7–C4, C4–C5
45	1266.9	0.52	2.68	4, 5t, 6t	26	907.46	142.75	9.74	2r
44	1257.83	2.30	3.41	6r, 7r					
Methylene-camphor									
62	1520.15	11.54	4.22	7, 3b, 5b, 6b	43	1250.79	0.81	-0.81	5t, 6t
61	1509.86	26.34	-13.48	7, 5b, 6b	42	1224.56	12.89	0.79	3t, 6t, 7
60	1504.67	2.06	-0.23	7, 5b, 1	41	1212.63	1.12	-3.08	?
59	1502.8	4.22	-1.78	7, 1	40	1194.4	1.59	-1.27	?
58	1491.26	10.53	-2.51	7, 3b, 5b, 6b, 1	39	1176.12	8.52	-7.31	?
57	1488.22	22.63	11.17	7, 3b, 5b, 6b, 1	38	1159	12.15	-1.25	?
56	1483.4	26.78	4.48	7, 3b, 5b, 6b, 1	37	1146.98	12.17	2.13	C1–C3
55	1476.32	6.01	0.78	7, 3b, 6b, 1	36	1119.11	7.04	-11.03	3t, 4, 5, 6
54	1470.04	8.66	1.57	7, 3b, 5b, 6b	35	1095.55	10.94	23.91	?

TABLE 1 (Continued)

no.	ω	D	R	assignment	no.	ω	D	R	assignment
Methylenecamphor (Cont'd)									
53	1435.49	12.68	-3.16	=CH2 b	34	1042.42	1.56	2.35	3w, 4, 5r
52	1415.21	40.74	2.78	7, 1	33	1032.08	2.35	-5.39	4, 3r, 5w, 6t
51	1400.2	19.22	-0.43	1	32	1003.01	0.54	2.51	7
50	1394.99	21.92	1.67	7	31	971.23	4.90	1.56	C5-C6
49	1347.16	7.70	-11.48	6r	30	962.52	1.52	-3.17	7, 1w, 5t, 6w
48	1328.95	3.85	-4.25	5r	29	955.71	8.21	0.59	7
47	1320.82	0.02	-0.78	4	28	947.12	11.17	-20.29	?
46	1303.79	2.78	0.30	3, 5, 6	27	927.51	2.94	3.29	C7-C4
45	1275.69	2.89	-4.08	3r, 5, 6	26	925.34	3.27	8.31	C1-C2
44	1268.81	1.46	3.83	3r	25	902.2	149.90	7.65	=CH2 r

^a DFT calculations performed by Gaussian 03 (see text). Numbers in the assignment lists refer to chemical groups; letters have the following meanings: b = bend; r = rock; t = twist; w = wag. Single numbers correspond either to CH₃ groups or to CH₂ groups where a single H is moving; modes without a dominant motion, i.e., modes whose energy is spread out over the whole molecule are denoted by a question mark. The first column is the numbering proposed by GAUSSIAN ordered by increasing frequency.

TABLE 2: Calculated Frequencies ω (cm⁻¹), Dipole Strengths D (10⁻⁴⁰ esu² cm²), Rotational Strengths R (10⁻⁴⁴ esu² cm²) and Mode Assignments for Fenchone, Methylenefenchone, Camphor, and Methylenecamphor in the Region 3050–2800 cm⁻¹ ^a

no.	ω	D	R	assignment	no.	ω	D	R	assignment
Fenchone									
75	3131.126	25.2676	-4.7633	3	67	3096.18	18.2971	-26.9933	4, 5, 6a
74	3127.432	36.7297	-14.0368	3	66	3092.569	46.202	12.7109	4
73	3119.525	45.4629	-14.6269	5a	65	3066.179	47.0876	31.7381	5s
72	3118.725	19.7255	3.3974	1	64	3056.885	37.3725	-9.1429	7s
71	3115.938	42.6515	105.77	3	63	3052.088	38.7663	-20.8639	6s
70	3113.861	16.402	-60.9262	3	62	3040.91	33.7208	0.3148	3
69	3110.969	23.8162	25.7066	1	61	3037.962	35.7346	2.1629	1
68	3107.541	13.0514	-38.0749	7a	60	3037.045	25.1997	5.3486	3
Camphor									
75	3134.114	31.6823	4.6737	7	67	3097.192	7.7953	23.9967	4, 5a, 6a
74	3122.071	25.7027	-7.5398	7, 3a	66	3092.994	36.5346	4.3387	4
73	3119.041	21.4172	-7.9829	1	65	3069.14	41.2331	-22.6157	4, 5s, 6s
72	3116.126	73.6898	41.7325	1, 5a, 6a	64	3066.629	16.8975	5.253	3s
71	3114.732	12.0925	-56.2801	1, 5a, 6a	63	3059.582	33.9331	3.155	5s, 6s
70	3108.639	5.9482	-7.9682	3a	62	3041.951	45.6951	11.6851	1, 7
69	3104.868	58.2208	6.8924	7	61	3039.347	28.6078	-14.7601	1, 7
68	3099.024	6.3434	0.3681	7	60	3035.648	19.7342	1.1865	7
Methylenefenchone									
81	3218.929	14.9658	1.1988	=CH2 a	72	3099.732	21.7743	12.0434	1
80	3139.234	13.8016	-1.6907	=CH2 s	71	3096.174	6.5238	-16.7144	5, 6a
79	3128.157	27.8695	-7.9571	3	70	3088.884	56.9678	11.4413	4
78	3124.668	42.4571	-14.9159	3, 7	69	3061.939	63.2207	32.4768	5s
77	3117.606	56.1237	16.1391	5a, 6a	68	3052.078	41.7452	-18.0624	7s
76	3110.175	62.8804	99.8818	1, 3, 7a	67	3045.153	45.8508	-9.1528	6s
75	3107.255	7.5456	-23.9353	1	66	3034.285	49.5896	-0.6072	7s
74	3104.466	47.7314	-89.8024	3	65	3030.244	33.8236	10.3184	1s
73	3100.05	18.5945	10.1325	3	64	3030.078	26.3635	-8.1585	7
Methylenecamphor									
81	3220.243	13.6053	0.115	=CH2 a	72	3093.927	12.7454	-3.0897	3a, 4, 5a, 6a
80	3138.286	14.2617	-1.2114	=CH2 s	71	3088.969	28.7128	80.5896	3a, 4, 5a
79	3130.334	31.4474	4.6977	7	70	3087.517	39.5356	-60.6026	3a, 4
78	3127.576	31.5507	-5.9336	7	69	3061.559	51.647	-27.7792	5s, 6s
77	3111.336	38.6301	52.9576	1	68	3051.788	42.7662	16.1363	5s, 6s
76	3109.483	65.1179	-76.3836	1, 5a, 6a	67	3051.02	28.302	7.9751	3s
75	3102.299	19.6114	-2.896	1, 7	66	3038.885	62.7222	-5.8408	1, 7
74	3099.271	73.583	5.6968	1, 7	65	3033.812	25.6064	1.9926	1, 7
73	3094.43	2.9688	17.2715	7	64	3032.98	22.5756	-1.6233	1, 7

^a DFT calculations performed by Gaussian 03 (see text). Numbers in the assignment lists refer to chemical groups; letters have the following meanings: s = symmetric; a = antisymmetric. These labels are attached solely to CH₂ groups and describe the relative motion of the atoms within the group. The symbol =CH₂ stands for the olefin group. Single labels correspond to CH₃ groups (the motion being a stretch in all cases). The first column is the numbering proposed by GAUSSIAN ordered by increasing frequency.

is a quite narrow, slightly asymmetric band observed at ca. 1190 nm. The calculations are in line with these results, except that the narrow main absorption band is calculated 10 nm lower than experimental, i.e., at ca. 1180 nm: this is due to the chosen values for the anharmonicity constants χ , which are assumed

to be close to experimental values, as discussed above. The evident weak band observed for all camphors at ca. 1140 nm is not calculated in our model, which allows for the existence of just (3, 0) local modes. It is then attributed to (2, 1) combinations, because, by assuming $\omega_0 = 3080$ cm⁻¹ (see Table 3) and

TABLE 3: Calculated Anharmonic Wavelengths λ (nm) for the $\Delta\nu = 3$ Region, Harmonic Frequencies ω (cm^{-1}), Dipole Strengths D (10^{-40} esu² cm²) and Rotational Strengths R (10^{-44} esu² cm²) for FEN, MEFEN, CAM, MECAM^a

fenchone				methylenefenchone				camphor				methylenecamphor							
group	λ	ω	D	R	group	λ	ω	D	R	group	λ	ω	D	R	group	λ	ω	D	R
6	1184.9	3073.1	34.8	-3.66	6	1189.5	3062.2	50.6	-7.88	7	1182.9	3077.8	36.8	0.95	6	1185.7	3071.4	44.3	0.30
7	1183.1	3077.4	40.3	-4.64	7	1185.9	3070.8	51.5	1.11	7	1181.7	3080.9	35.8	-5.58	7	1183.7	3076.1	41.7	-7.51
5	1182.9	3077.8	44.7	6.11	3	1185.6	3071.4	43.6	-7.44	6	1181.2	3082.1	28	4.18	7	1183.4	3076.7	40.5	0.41
3	1180.8	3083.0	34.1	-6.1	5	1185.5	3071.7	51.8	5.67	5	1179.6	3085.8	43.8	-4.12	7	1181.5	3081.3	35.9	-6.36
3	1180.4	3083.9	34.8	1.91	3	1184.6	3073.8	48.1	0.18	6	1179.3	3086.5	30.3	-1.42	5	1181.4	3081.4	48.1	-3.64
6	1180.3	3084.2	27.2	-3.63	1	1182.0	3080.1	30.8	8.70	7	1178.6	3088.2	31.6	-5.59	7	1181.3	3081.7	36.4	9.46
1	1179.0	3087.3	36.1	-0.18	1	1180.1	3084.7	38.0	-1.68	3	1178.2	3089.1	17.6	-6.68	1	1181.2	3081.9	31.4	7.79
4	1177.5	3090.8	47.3	-1.12	4	1179.1	3086.9	54.7	1.06	7	1177.9	3089.9	30.6	6.21	5	1179.4	3086.3	47.7	-7.28
1	1175.5	3095.6	28.4	-4.1	6	1177.8	3090.1	30.5	1.06	1	1177.7	3090.3	30.4	-3.06	3	1179.2	3066.8	36.1	-6.11
7	1174.6	3097.9	35.2	3.09	3	1177.1	3091.8	31.7	8.39	4	1177.0	3092.0	47.6	-1.05	4	1178.8	3087.7	56.4	1.36
1	1172.1	3103.9	19.4	4.02	1	1176.9	3092.2	30.3	-7.87	3	1176.6	3092.9	13.5	5.86	1	1178.3	3088.9	32.5	-3.87
3	1170.3	3108.2	20.9	-7.87	3	1175.2	3096.5	30.1	-6.52	5	1176.2	3093.9	39.6	-5.62	3	1177.8	3070.1	30.2	14.90
3	1170.1	3108.7	19.9	7.18	7	1173.1	3101.4	37.5	0.16	1	1174.5	3098.2	25.6	-1.38	1	1177.0	3092.0	27.6	-5.30
3	1168.9	3111.6	29.7	0.63	5	1169.3	3110.8	37.8	2.55	1	1171.8	3104.6	19.1	3.43	6	1175.9	3094.6	33.9	2.73
3	1168.1	3113.7	29.1	4.63	3	1168.9	3111.6	29.9	0.54	7	1168.9	3111.6	25.2	0.66	7	1163.4	3125.0	22.6	0.66
5	1167.9	3114.2	34.7	2.36	3	1167.5	3115.0	28.7	4.02	7	1161.7	3129.2	28.2	0.93	7	1161.8	3129.2	29.8	2.84
					=CH	1124.2	3184.9	16.9	0.75						=CH ₂	1124.8	3183.5	19.7	0.09
					=CH	1120.0	3196.2	14.7	1.27						=CH ₂	1119.5	3197.5	13.1	0.34

^a In the first column for each molecule we provide the number of the groups to which the local CH-stretching belongs. The olefin CHs are indicated as =CH.

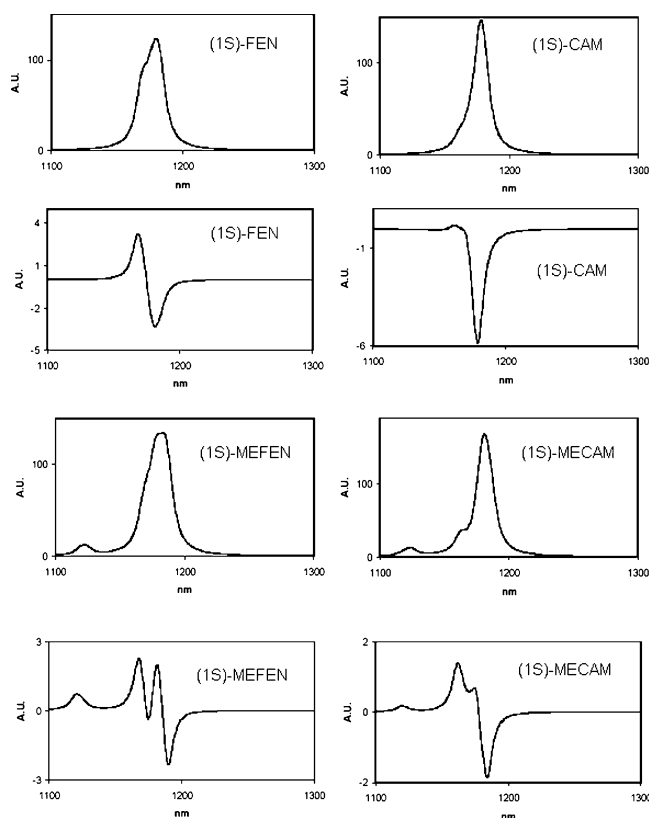


Figure 6. Calculated absorption and VCD spectra in the NIR (1300–1100 nm) of (1*S*)-fenchone (FEN) (top left), of (1*S*)-camphor (CAM) (top right), of (1*S*)-2-methylenefenchone (MEFEN) (bottom left), and of (1*S*)-2-methylenecamphor (MECAM) (bottom right). Calculations were performed as explained in the text.

$\chi = 65 \text{ cm}^{-1}$, one has from the Birge–Sponer law¹⁸ $\omega_{\text{comb}} = 2(\omega_0 - \chi) - 4\chi + (\omega_0 - \chi) - \chi = 3\omega_0 - 8\chi = 8720 \text{ cm}^{-1}$, i.e., $\lambda_{\text{comb}} = 1150 \text{ nm}$. The olefin CH local modes that are observed at ca. 1115 nm in MECAM are predicted by the present calculations at ca. 1125 nm. All this is not too bad at all and in conclusion we may say that the cage-type structure of these bridged bicyclic rigid compounds gives rise to a sort of degeneracy that is partially relieved by substituting the C=O group with C=CH₂. These same effects are even more evident

for FEN and MEFEN; especially for MEFEN the main observed absorption peak should rather be called a doublet at 1195 and 1185 nm, which are matched by calculations, except that the prediction is again for generally lower wavelengths, the calculated ω_0 being “too harmonic” or the chosen anharmonicity constant being a bit too low. The rest of the features is attributed in the same way as in the case of camphor compounds (see Figures 5 and 6). In both cases the shape of the absorption spectra is also determined by calculated dipole strengths which may evidently be considered acceptable. This means that probably for hydrogen atoms the electrical anharmonic terms beyond the APT’s are dependent on the chemical environment in a similar way as the APT’s themselves (see, e.g., ref 21).

Let us now come to the discussion of the NIR–VCD results and let us say at the beginning that here the comparison of experiments and calculations is not as satisfactory as in the NIR-absorption case. This may have several causes: “transferring” or rather using AATs disregarding anharmonic corrections is not as possible as for APTs;⁹ also VCD may require a less crude approximation than the local mode one. From Figure 5, we observe that the (1*S*)-CAM and (1*S*)-MECAM exhibit a negative feature at high wavelengths (ca. 1190 nm) followed by a positive band at low wavelengths, the relative importance of the + and – components is quite different in CAM and MECAM. Instead, the (1*S*)-enantiomers of FEN and MEFEN exhibit two closely negative VCD features between 1195 and 1180 nm (resolved in the second case). For both (1*S*)-FEN/MEFEN and (1*S*)-CAM/MECAM the calculations bear a common general (–, +) aspect in decreasing order of wavelengths, which makes the results not fully satisfactory, especially for FEN and CAM. The calculated NIR–VCD spectra look more acceptable for MECAM and MEFEN and this allows us to make a tentative assignment of the observed features, accepting the indications of Table 3. The negative feature for (1*S*)-MECAM calculated at ca. 1180 nm receives major contributions from local modes located in the bridge methyls, as well as in the methyl at **1**, of local modes at **5** and **3**; the positive feature calculated at ca. 1170 nm is principally due to local modes at **3** and again to bridge methyl CHs. In (1*S*)-MEFEN the negative feature at ca. 1180 nm is due to local modes in the geminated methyls in **3** and to local modes in **5** and **6**. This feature is followed by a positive feature at ca. 1175 nm containing contributions from the CH₃ in **1**, and

from **6** and **4***. Then we have calculated a faint negative feature at ca. 1170 nm containing contributions from the CH₃ in **3** and **1**. The last feature, due to aliphatic local modes at **5** and in the CH₃ at **3**, is positive and is calculated at ca. 1165 nm. More or less the same assignment can be made for the calculated features of the CAM and FEN molecules, except for the local modes at **3** in camphor (see Table 3). Besides, the correspondence with experimental data in Figure 5 is not as nice. For both MECAM and MEFEN the olefin local modes at ca. 1120 nm are calculated to have a positive VCD, as observed. Of course in the present calculations there is no possibility of calculating combinations modes that are observed at ~1140 nm and we have thus no explanation for the fact that such combination VCD features are negative for (1*S*)-CAM and (1*S*)-FEN, positive for (1*S*)-MECAM and either negative or bisigned negative/positive for (1*S*)-MEFEN. As in the case of the fundamental CH-stretchings region, we notice that the shapes of the calculated VCD bands are largely due to superpositions of nearby lines, which often are oppositely signed: this makes a detailed attribution of each observed feature still impossible. The message arising out of these spectra, however, is that the NIR-VCD spectra of FEN and MEFEN and of CAM and MECAM, respectively, are related in pairs: indeed, the NIR-VCD spectra of the olefins resemble, to some extent, the same spectra as those of the corresponding ketones, with just a better resolution. This correspondence has been observed also in the fundamental CH-stretching region, where VCD spectra are determined by the chiral arrangement of CH₂/CH₃ groups in the cage structure of these [2.2.1] bridged molecules, rather than to the chemical function in position **2**. Unlike the case of the fundamental CH-stretching region, we do not notice here an overall inversion in sign of the whole VCD spectra. When comparing camphor type with fenchone type molecules: the band at ca. 1184 nm in (1*S*)-FEN has the aspect of an unresolved (–, –) doublet, which is seen more precisely in (1*S*)-MEFEN, with the (–, –) components at 1195 and 1183 nm; this doublet in CAM and MECAM is (–, +) with components at 1193 and 1179 nm and 1190 and 1168 nm, respectively. So the lower wavelength/higher frequency components seem to be inverting and can be attributed from calculation to CH₃ local modes in position **3** in FEN and MEFEN and to CH₃ local modes in position **7** in CAM and MECAM (compare with the CH-stretching fundamental region); the higher wavelength contributions to VCD instead are negative for all *S* compounds and their sign is reproduced by calculations.

IV. Summary and Conclusions

We have obtained and analyzed the VCD spectra of the enantiomers of fenchone, camphor, 2-methylenefenchone, and 2-methylenecamphor. The VCD spectra were measured in three different spectral regions: the mid-IR deformation region between 900 and 1500 cm⁻¹; the IR region of CH-stretching fundamentals between 2700 and 3100 cm⁻¹; and the NIR region of CH-stretching second overtones between 7700 and 9100 cm⁻¹ (1300–1100 nm). The interpretation of the spectra was made by use of DFT calculations performed with GAUSSIAN03. The comparison of the VCD data of olefins and corresponding ketones has allowed us to draw a few interesting conclusions:

(1) The presence of the C=O or C=CH₂ group in position **2** affects a well defined and limited part of the VCD spectrum in the mid-IR region; this influence is well manifested in the CC-stretching region for those CC-bonds close to the C=O (C=CH₂) group.

(2) The influence of the C=O/C=CH₂ groups on the IR-VCD CH-stretching fundamental spectra and on the NIR-VCD

overtone spectra appears almost irrelevant. The spectra in this region appear to be determined mainly by the chiral arrangement of CH₂, CH₃, and C*H groups, which is the same in FEN and MEFEN and is the same in CAM and MECAM. The observed (and reproduced by calculations) opposite behavior of FEN and CAM as well as that of MEFEN and MECAM, which is particularly evident in the IR CH-stretching fundamental VCD spectra, is attributed to a submoiety of the bicyclic structure having enantiomeric geometry in FEN and CAM.

Both (1) and (2) are subject to future verification and will attract our efforts. Conclusion 2 above has some potential use in the determination of the absolute configuration (AC) of molecules. The part of the VCD spectrum in the fundamental CH stretching region for frequencies higher than 2900 cm⁻¹ can be used together with reliable DFT calculation to predict the AC, as currently done in the MID-IR (with the advantage of using less substance and even quartz cells). For this reason we suggest investigation of the VCD spectra of related molecules of natural origin, like borneol, thiocamphor, fenchyl alcohol, etcetera, as well as of synthetic origin: common motifs may be found for a minimal moiety of the large one indicated in the Discussion. Otherwise, one may hope to define the perturbations by substituent groups in the various positions that can turn out to be useful both in the determination of AC and for the synthetic chemist. About NIR-VCD, because a truly a priori method to calculate spectra needs further theoretical developments, a correlative study is also needed in support.

Acknowledgment. Italian Ministry of Education, University and Research (through two different COFIN 2004 programmes), and EULO, Brescia, are thanked for financial support. We also acknowledge help and assistance from Ettore Castiglioni.

References and Notes

- (1) Lightner, D. A.; Gurst, J. *Organic Conformational Analysis and Stereochemistry from Circular Dichroism Spectroscopy*; Wiley-VCH: New York, 2000.
- (2) Coulombeau, C.; Rassat, A. *Bull. Soc. Chim. Fr.* **1966**, *12*, 3752.
- (3) Kirk, D. N. *J. Chem. Soc., Perkin Trans.* **1977**, 2122.
- (4) Pulm, F.; Schramm, J.; Hormes, J.; Grimme, S.; Peyerimhoff, S. *D. Chem. Phys.* **1997**, *224*, 143.
- (5) Pulm, F.; Schramm J.; Lagier H.; Hormes, J. *Enantiomer* **1998**, *3*, 315.
- (6) Giorgio, E.; Viglione, R. G.; Zanasi, R.; Rosini, C. *J. Am. Chem. Soc.* **2004**, *126*, 12968.
- (7) Devlin, F. J.; Stephens, P. J.; Cheeseman, J. P.; Frish, M. J. *J Phys Chem A* **1997**, *101*, 6322.
- (8) Nafie, L. A. In *Advances in Infrared and Raman Spectroscopy*; Clark, R. J. H., Hester, R. E., Eds.; J Wiley: New York, 1984; Chapter 2, p 49.
- (9) Stephens, P. J. *J. Phys. Chem.* **1985**, *89*, 748. Stephens, P. J.; Lowe, M. A. *Ann. Rev. Phys. Chem.* **1985**, *36*, 213. Stephens, P. J.; Devlin, F. J.; Chabalowski, C. F.; Frisch, M. J. *J. Phys. Chem.* **1994**, *98*, 11623.
- (10) Polavarapu, P. L. In *Vibrational Spectra and Structure*; Elsevier: Amsterdam, 1989; Vol. 17B, pp 319–342.
- (11) Keiderling, T. A. In *Circular Dichroism, Principles and Applications*; Berova, N., Nakanishi, K., Woody, R. A., Eds.; Wiley-VCH: New York, 2000; Chapter 22.
- (12) Frisch, M. J.; Trucks, G. W.; Schlegel, H. B.; Scuseria, G. E.; Robb, M. A.; Cheeseman, J. R.; Montgomery, J. A., Jr.; Vreven, T.; Kudin, K. N.; Burant, J. C.; Millam, J. M.; Iyengar, S. S.; Tomasi, J.; Barone, V.; Mennucci, B.; Cossi, M.; Scalmani, G.; Rega, N.; Petersson, G. A.; Nakatsuji, H.; Hada, M.; Ehara, M.; Toyota, K.; Fukuda, R.; Hasegawa, J.; Ishida, M.; Nakajima, T.; Honda, Y.; Kitao, O.; Nakai, H.; Klene, M.; Li, X.; Knox, J. E.; Hratchian, H. P.; Cross, J. B.; Bakken, V.; Adamo, C.; Jaramillo, J.; Gomperts, R.; Stratmann, R. E.; Yazyev, O.; Austin, A. J.; Cammi, R.; Pomelli, C.; Ochterski, J. W.; Ayala, P. Y.; Morokuma, K.; Voth, G. A.; Salvador, P.; Dannenberg, J. J.; Zakrzewski, V. G.; Dapprich, S.; Daniels, A. D.; Strain, M. C.; Farkas, O.; Malick, D. K.; Rabuck, A. D.; Raghavachari, K.; Foresman, J. B.; Ortiz, J. V.; Cui, Q.; Baboul, A. G.; Clifford, S.; Cioslowski, J.; Stefanov, B. B.; Liu, G.; Liashenko, A.; Piskorz, P.; Komaromi, I.; Martin, R. L.; Fox, D. J.; Keith, T.; Al-Laham, M. A.; Peng, C. Y.; Nanayakkara, A.; Challacombe, M.; Gill, P. M. W.;

Johnson, B.; Chen, W.; Wong, M. W.; Gonzalez, C.; Pople, J. A. *Gaussian 03*, revision B.05; Gaussian, Inc.: Pittsburgh, PA, 2003.

(13) Lightner, D. A.; Flores, M. J.; Crist, B. V.; Gawronski, J. K. *J. Org. Chem.* **1980**, *45*, 3518.

(14) Devlin, F. J.; Stephens, P. J.; Cheeseman, J. R.; Frisch, M. J. *J. Phys. Chem.* **1997**, *101*, 9912–9924.

(15) Castiglioni, E.; Lebon, F.; Longhi, G.; Abbate, S. *Enantiomer* **2002**, *7*, 161.

(16) Longhi, G.; Gangemi, R.; Lebon, F.; Castiglioni, E.; Abbate, S.; Pultz, V. M.; Lightner, D. A. *J. Phys. Chem. A* **2004**, *108*, 5338.

(17) Cao, X.; Shah, R. D.; Dukor, R. K.; Guo, C.; Freedman, T. B.; Nafie, L. A. *Appl. Spectrosc.* **2004**, *58*, 1057.

(18) Henry, B. R. *Acc. Chem. Res.* **1987**, *20*, 429. Child, M. S.; Halonen, L. *Adv. Chem. Phys.* **1985**, *LVII*, 1.

(19) Child, M.; Halonen, L. *Adv. Chem. Phys.* **1985**, *LVII*, 1.

(20) Henry, B. R. *Acc. Chem. Res.* **1987**, *20*, 429.

(21) Longhi, G.; Zerbi, G.; Ricard, L.; Abbate, S. *J. Chem. Phys.* **1988**, *88*, 6733.

(22) Kjaergaard, H. G.; Henry, B. R. *J. Chem. Phys.* **1992**, *96*, 4841.

(23) Gangemi, R.; Longhi, G.; Lebon, F.; Abbate, S.; Laux, L. *Monatsh. Chem.* **2005**, *136*, 325.

(24) Abbate, S.; Longhi, G.; Santina, C. *Chirality* **2000**, *12*, 180.

(25) Fang, H. L.; Swofford, R. L.; McDevitt, M.; Anderson, A. B. *J. Phys. Chem.* **1985**, *89*, 225.

(26) Turnbull, D. M.; Kjaergaard, H. G.; Henry, B. R. *Chem. Phys.* **1995**, *195*, 129.

(27) Rong, Z.; Henry, B. R.; Robinson, T. W.; Kjaergaard, H. G. *J. Phys. Chem. A* **2005**, *109*, 1033.

(28) Devlin, F. J.; Stephens, P. J.; Besse, P. *J. Org. Chem.* **2005**, *70*, 2980.

(29) University of Brescia, unpublished results.

(30) Back, D. M.; Polavarapu, P. L. *Carbohydr. Res.* **1984**, *133*, 163.

(31) Toriguchi, T.; Miura, N.; Nishimura, S.; Monde, K. C. D. *Conference, Destin FL, August 21–25, 2005*; 2005; Poster 26.

(32) Abbate, S.; Havel, H. A.; Laux, L.; Pultz, V.; Moscovitz, A. *J. Phys. Chem.* **1988**, *92*, 3302.

(33) Laux, L.; Pultz, V. M.; Abbate, S.; Havel, H. A.; Overend, J.; Moscovitz, A.; Lightner, D. A. *J. Am. Chem. Soc.* **1982**, *104*, 4276.

(34) Moscovitz, A.; Lightner, D. A.; Pultz, V. M. The University of Minnesota, unpublished data, 1982.